Numerical CFD modelling of non-neutral atmospheric boundary layers for offshore wind resource assessment based on Monin-Obukhov theory

J. Sanz Rodrigo, D. Cabezón, I. Martí
CENER, Nacional Renewable Energy Centre (Spain)
jsrodrigo@cener.com
dcabezon@cener.com
imarti@cener.com

P. Patilla, J. van Beeck
VKI, von Karman Institute for Fluid Dynamics (Belgium)
patilla@vki.ac.be,
vanbeeck@vki.ac.be

Abstract

The presented works aim at proposing a methodology for the simulation of offshore wind conditions using CFD. The main objective is the development of a numerical model for the characterization of atmospheric boundary layers of different stability levels, as the most important issue in offshore wind resource assessment. Based on Monin-Obukhov theory, the steady k-ε Standard turbulence model is modified to take into account thermal stratification in the surface layer. The validity of Monin-Obukhov theory in offshore conditions is discussed with an analysis of a three day episode at FINO-1 platform.

1. Introduction

Offshore wind resource assessment at micrometeorological level has been most commonly carried out with linear models like WAsP, from RISO National Laboratory (Denmark). They are still the standard wind resource assessment tool in the wind industry. Even though the model was developed for neutral atmosphere over uniform terrain, it has been also used in other conditions such as complex terrain or offshore. The higher demands of the wind industry together with an important decrease of computational costs have brought the attention to more sophisticated models based on computational fluid dynamics (CFD).

A very significant increase on the number of papers related to CFD modelling has been observed in past EWECs, devoted to the simulation of complex terrain winds [4][11] or flow around forests edges [5]. So far, there is no consensus on a standard methodology for CFD modelling in wind energy applications. Only in Wind Engineering some general guidelines can be found [10], more related to the application to pedestrian level winds and wind loading on buildings. In general, the state of the art of CFD wind resource assessment shows two distinct philosophies: one based on steady-state RANS (Reynolds Averaged Navier-Stokes) turbulence models, and another one based on unsteady LES (Large-Eddy Simulation). The first one requires much less computational effort but involves more important simplifications. LES based models are more physically meaningful but the computational cost is also significantly higher. Hence RANS models are currently the state-of-the-art in operational wind resource assessment and LES models remain at academic level and can be considered as the next generation of CFD wind resource assessment. The modelling methodology presented in this paper is situated in the RANS family. Fluent 6.3 commercial CFD solver has been used [9]. The basic formulation of the model will be discussed and a test case will be presented.

The wind offshore differs from onshore conditions in two fundamental aspects: the roughness is not uniform as it depends on wind speed, and thermal stratification effects are predominant.

The surface roughness offshore is low compared to onshore conditions. That is why high winds develop on the sea. However, roughness depends on the wave field, which in turn depends on wind speed, distance to coast (fetch) and water depth.

The atmospheric stability offshore is governed by the large heat capacity of the sea. The atmospheric stability is present in the form of vertical momentum transport, which strongly influences the vertical wind profile. Stability effects have been commonly treated onshore using the Monin-Obukhov theory. The correction of the neutral atmospheric boundary layer with the Monin-Obukhov length is also the basis of WAsP modelling offshore [7].

With long fetches the flow develops equilibrium conditions and M-O theory should work reasonably well. However, when the wind blows from the land towards the sea, the coast introduces an important change in roughness and heat flux in the form of an internal boundary layer. The land-sea flow discontinuity can be present within distances of up to 100-200 km. If warm air flows over a cold sea a stable internal boundary layer develops, which is characterized by low turbulence with, therefore, low mixing of momentum and heat transfer. In these conditions, M-O theory does not apply as the flow is not in equilibrium.

Measurements at FINO-1 offshore platform, 45km off the German coast, are used to assess the validity of M-O theory under very stable and unstable offshore conditions. It will be shown that the theory reproduces the mean velocity profile reasonably well in unstable conditions but cannot predict the wind profile under very stable coastal wind conditions.

2. The model

The model follows the methodology developed by Masson et al. [1]: Standard k-ε turbulence model, under gravitational influence, is parameterized in order to be in equilibrium with Monin-Obukhov theory. Such theory is considered universally valid in the surface layer under homogeneous and stationary flow conditions. A priori, the theory is specially suited for offshore winds, considering the homogeneity of the sea surface compared to typical onshore conditions.

It is questionable whether this theory still applies at wind turbine heights of the order of 100m, where the wind profile is likely to be beyond the surface layer, especially under stable conditions. Based on measurements in Rodsand offshore mast in the Baltic Sea, Lange et al. [6] found systematic deviations from M-O theory on velocity profiles in near neutral and stable conditions, with a fetch of 30km. The deviations were attributed to the presence of coastal effects. A correction of the M-O theory, introducing the inversion height as an additional scaling parameter, provided better predictions in these situations.

The proposed modelling methodology is based on M-O theory as a widely recognized basis of surface layer meteorology. The intention is not to provide a universally valid model but rather to establish a comprehensive methodology that can be adapted to the particular local meteorology of a site. The CFD modelling strategy can be summarized as follows:

- Inlet homogeneous boundary conditions are defined according to measured roughness and stability conditions.
- Wall boundary conditions are prescribed according to roughness and local friction velocity (both related dynamically in offshore conditions) and surface temperature (or heat flux).
- Top boundary conditions are prescribed at a sufficiently high level such that the influence from the ground is not significant.
- Outlet and side boundaries should be sufficiently far to avoid any influence in the area of interest.
- The turbulence model parameterization is such that, under homogeneous flow over flat terrain, it is in equilibrium with inlet, top and wall boundary conditions. In other words, the inlet wind conditions are maintained downstream with negligible streamwise gradients throughout the domain.

2.1 Standard k-ε model

CFD modelling using RANS Standard k-ε model has been a popular choice in Wind Engineering because of its robustness, economy and reasonable accuracy. A survey of this and other RANS models can be found in [4]. In these models the Reynolds shear stresses are modelled using the Boussinesq approximation, which relates them with the velocity gradients through the turbulent viscosity μ_t. In the Standard k-ε model, turbulence is considered isotropic and the turbulence viscosity is obtained from the solution of the transport equations for turbulent kinetic energy (k) and turbulent dissipation rate (ε). In steady-state incompressible conditions:

$$\mu_t = \rho C_\mu \frac{k^2}{\varepsilon} \tag{1}$$

$$\frac{\partial}{\partial x_i}(\rho k u_i) = \frac{\partial}{\partial x_j}\left((\mu + \frac{\mu_t}{\sigma_k}) \frac{\partial k}{\partial x_j} \right) + \tag{2}$$
$$+ G_k + G_b - \rho\varepsilon$$

$$\frac{\partial}{\partial x_i}(\rho \varepsilon u_i) = \frac{\partial}{\partial x_j}\left((\mu + \frac{\mu_t}{\sigma_k}) \frac{\partial \varepsilon}{\partial x_j} \right) + \tag{3}$$
$$+ C_{1\varepsilon} \frac{\varepsilon}{k}\left(G_k + (1 - C_{3\varepsilon}) G_b \right) - C_{2\varepsilon} \frac{\varepsilon^2}{k} \rho$$

$C\mu$=0.09, $C_{1\varepsilon}$=1.44, $C_{2\varepsilon}$=1.92, σ_k=1 and σ_ε=1.3 are the default constants of the Jones and Launder (1972) k-ε model implemented in Fluent 6.3 [9]. G_k and G_b are the production of turbulent kinetic energy by shear and buoyancy effects.

$$G_k = \mu_t \left(\frac{\partial u_i}{\partial x_j} + \frac{\partial u_j}{\partial x_i} \right) \frac{\partial u_i}{\partial x_j} \tag{4}$$

$$G_b = \beta g \frac{\mu_t}{\sigma_t} \left(\frac{\partial T}{\partial x_i} - \frac{g_i}{Cp} \right) \tag{5}$$

where β is the thermal expansion coefficient of air and g/Cp is the adiabatic lapse rate. If the temperature gradient is larger than g/Cp, G_b>0 and turbulence will be generated by buoyancy effects (unstable conditions). If, the temperature gradient is lower than the adiabatic lapse rate, turbulence will be attenuated by buoyancy effects (stable conditions).

The momentum and energy equations include gravity effects. The Boussinesq approximation for density assumes that the temperature (density) variations are small and only depend on temperature (linearly through the expansion coefficient) in the buoyancy terms.

2.2 Inlet Conditions

In k-ε models, it is necessary to prescribe the inlet profiles of velocity, temperature, turbulent kinetic energy and turbulent dissipation rate. In the surface layer, the vertical variations of shear stress, heat and moisture fluxes are roughly constant. In homogeneous and stationary conditions the wind velocity and potential temperature θ variation with height follow a similar log-law with scaling parameters L, $u*$ and $T*$ according to M-O similarity theory:

$$L = \frac{u_*^2 T_w}{\kappa g T_*}; \quad u_* = \sqrt{\frac{\tau_w}{\rho}}; \quad T_* = \frac{-q_w}{\rho C_p u_*} \tag{6}$$

$$\frac{U}{u_*} = \frac{1}{\kappa}\left[\ln\left(\frac{z}{z_0} \right) - \psi_m \left(\frac{z}{L} \right) \right] \tag{7}$$

$$\frac{\theta(z) - \theta_0}{T_*} = \frac{1}{\kappa}\left[\ln\left(\frac{z}{z_0} \right) - \Psi_h \left(\frac{z}{L} \right) \right] \tag{8}$$

$$\theta = T + \frac{g}{C_p} \Delta z \tag{9}$$

L is the M-O length, $u*$ is the friction velocity, τ_w is the wall shear stress, z_0 is the roughness length, T_w is the wall temperature and q_w is the wall heat flux (positive in unstable atmosphere, i.e. wall cooled by air). Ψ_m and Ψ_h are "universal" stability functions whose most popular forms are the ones from Businger-Dyer and Paulson [12].

Similarly, profiles for k and ε are obtained as functions of the nondimensional length z/L.

$$k = \frac{u_*^2}{\sqrt{C_\mu}} \left[\frac{\phi_\varepsilon\left(\frac{z}{L}\right)}{\phi_m\left(\frac{z}{L}\right)} \right]^{\frac{1}{2}} \tag{10}$$

$$\varepsilon = \frac{u_*^3}{\kappa z} \phi_\varepsilon \left(\frac{z}{L} \right) \tag{11}$$

From the temperature and velocity gradient, the M-O length can be computed through the gradient Richardson number [12].

$$Ri \approx \frac{g\left(\frac{\Delta T}{\Delta z}+\frac{g}{Cp}\right)}{T\left(\frac{\Delta U}{\Delta z}\right)^2} \quad (12)$$

where the temperature and velocity gradients are evaluated at two height levels, z_1 and z_2, and the effective height for the *Ri* is $z=(z_1-z_2)/\ln(z_1/z_2)$. The M-O length is computed as:

$$L=\begin{cases}\frac{z}{Ri} & Ri<0\ (unstable)\\ \frac{z(1-5Ri)}{Ri} & 0<Ri<0.2\ (stable)\end{cases} \quad (13)$$

Positive L values below 200m are typical of very stable conditions, negative *L* above -200m for very unstable and an absolute value of L above 1000 is considered as neutral conditions.

The M-O length depends on the choice of the two levels from which the *Ri* number is calculated. An overall value, characteristic of the wind turbine rotor area, is obtained from the 40 and 100 m levels. A wider separation between the two levels provides larger velocity and temperature gradients and, therefore, a more robust characterization of the stability.

The sensitivity of the roughness length on the wind profile is considerably less important than the thermal stratification [6]. The roughness length is linked to the friction velocity through the Charnock relation, for fully developed wave fields (open sea conditions).

$$z_0 = 0.0185\frac{u_*^2}{g} \quad (14)$$

Otherwise, a constant value of 0.2mm can be considered.

2.3 Wall Boundary Conditions

No slip (zero velocity) conditions are typical boundary conditions for momentum equations in wall bounded flows. Either Wall temperature or heat flux is prescribed as boundary condition for the energy (temperature) equation. Both are related through the local heat transfer coefficient *h*, which depends on the local flow field conditions:

$$q_w = h(T_w - T_p) \quad (15)$$

where subscript *p* refers to the near wall position (first grid cell). Turbulence quantities near the wall follow the assumption of local equilibrium, i.e., the production of turbulent kinetic energy equals the dissipation rate. In neutral conditions $G_k=\rho\varepsilon$ and:

$$k_p = \frac{u_*^2}{\sqrt{C_\mu}} \quad (16)$$

$$\varepsilon_p = \frac{u_*^3}{\kappa z_p} \quad (17)$$

Similarly, under thermal stratification equations (10) and (11) are evaluated at the first cell height z_p to prescribe the wall turbulence quantities.

Wall functions are used to make the link between the first cell and the wall boundary conditions. If standard turbulent law-of-the-wall is used for velocity, a necessary requirement, in order to obtain equilibrium between the wall shear stress and the ABL, is that the velocity of the law-of-the-wall equals the ABL log-law [3][4]. Otherwise, a different roughness length will be seen by the incoming velocity profile and an internal boundary layer will develop, deteriorating the flow homogeneity.

An alternative to the wall functions approach is to prescribe the flow conditions in the bottom layer of the domain. This is equivalent to defining the flow conditions at the roughness length level. The link between the roughness length layer and the flow is done by computing a local friction velocity according to (7) [2].

$$u_{*p} = \frac{U_p \kappa}{\ln\left[\frac{z_p}{z_0} - \psi_m\left(\frac{z_p}{L}\right)\right]} \quad (18)$$

2.4 Top Boundary Conditions

The top boundary should be placed well above the area of interest, up to a level where the flow conditions can be prescribed.

The most logical choice is the inversion height, where geostrophic wind conditions can be assumed. If the inversion height cannot be estimated, another possibility is to assume symmetry boundary conditions, which will ensure that the flow is parallel to the boundary.

In the present study, the objective is to simulate homogeneous surface layer profiles according to M-O theory. Hence, the inlet conditions are prescribed at the top layer height (300m in the test case), instead of the geostrophic drag law. This means that surface layer equations are also valid in the top boundary, and they remain undisturbed throughout the domain.

2.5 Outlet and side boundary conditions

Outlet and side boundary conditions are less important in ABL modeling. They should be sufficiently far away from the region of interest so that they don't affect the flow field of this area. Typically symmetry conditions are prescribed at the side boundaries and pressure outlet at the outlet boundary.

2.6 Model parameterization

The parameterization of the turbulent model is made such that, if homogeneous conditions are introduced in the inlet and there is no perturbation through the wall, side and top boundaries, the same flow conditions should be obtained at the domain outlet. In the case of ABL, M-O profiles are introduced in the k-ε equations to obtain a set of constants that satisfy this equilibrium requirement. In neutral conditions, the following conditions apply to k-ε model [13]:

$$C_\mu = 0.0333 \tag{19}$$

$$\sigma_\varepsilon \sqrt{C_\mu}\left(C_{2\varepsilon} - C_{1\varepsilon}\right) = \kappa^2 \tag{20}$$

The default parameterization of Launder and Jones does not comply with these requirements and, therefore, will deteriorate the homogeneity of the M-O flow.

In thermally stratified atmosphere, the stability functions introduce a dependency on *L* which has to be accounted for in the turbulence model. This is done by modifying the value of the $C_{3\varepsilon}$ constant in (3), which affects the production of turbulent kinetic energy due to buoyancy in the ε equation. Introducing the M-O expressions of *U*, *T*, *k* and *ε* in (3) a condition for $C_{3\varepsilon}$ is obtained that depends on *z*/*L*. The obtained analytical expression is approximated by Alinot and Masson by a fifth-order polynomial, function of *z*/*L* [1]. This expression approximates the near wall region to avoid excessive gradients in $C_{3\varepsilon}$ with height (Figure 1). A constant $C_{3\varepsilon}$, independent of height and based on local *L*, can also be used for the sake of simplicity: 4.5 for stable conditions and -2 for unstable conditions.

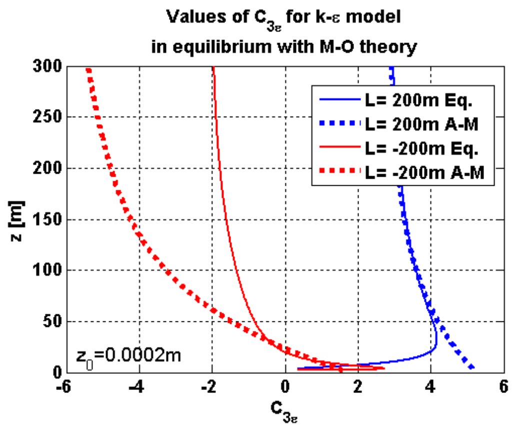

Figure 1: Values of C3ε for k-ε model in equilibrium with M-O theory. Comparison with Alinot and Masson function.

3. Test case

The above described CFD model is implemented in the solution of a stable boundary layer over open sea conditions. M-O profiles are used with a roughness length of 0.2mm and M-O length of 200m. The profile results in a friction velocity of 0.32m/s (9.2m/s and 7.1% turbulence intensity at 10m).

A grid sensitivity analysis is performed on the dependency on the near wall cell height. The grid resolution in the near wall region is important as it is the area with the largest temperature and velocity gradients, responsible for the turbulence characteristics of the surface layer. Figures 2 to 5 show a comparison between inlet and outlet *U*, *T*, *k* and turbulence intensity profiles on a 1000x300 m domain with three different first cell heights z_p: 0.1m, 0.5m and

1m. A boundary layer scheme is used to mesh the domain which gradually decreases the spatial resolution with height down to grid cells of 10m, which is maintained up till the top layer. The simulations are performed in 2D with 4000-6000 cells. A constant value of $C_{3\varepsilon}$=4.5 is used.

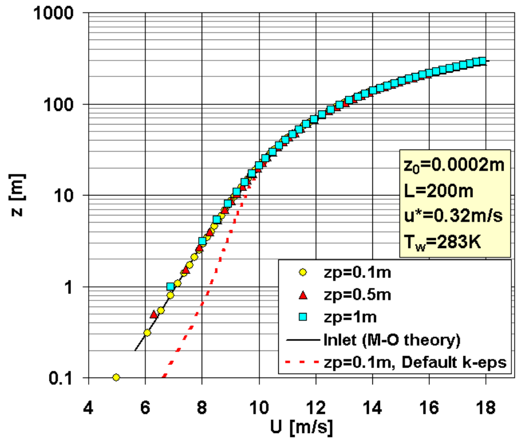

Figure 2: Near-wall grid sensitivity on velocity profile. Comparison with default model configuration.

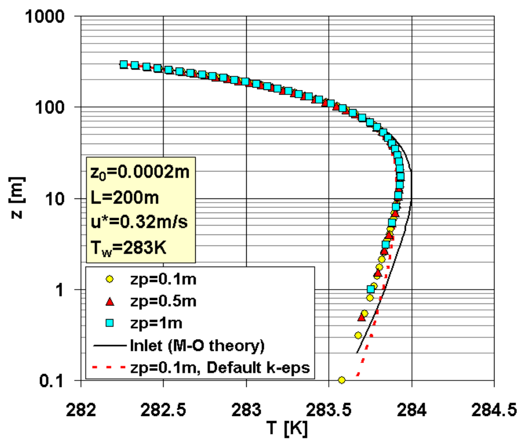

Figure 3: Near-wall grid sensitivity on temperature profile. Comparison with default model configuration.

It is noticed that increasing the grid resolution near the ground provides better results, especially in the turbulence intensity. Compare to the default model settings provided by Fluent 6.3, the accuracy of the new model is significantly improved. The default model, with smooth wall treatment, accelerates the flow near the ground and decreases the turbulence intensity. In the contrary, at hub height (100m) the turbulence intensity is overpredicted.

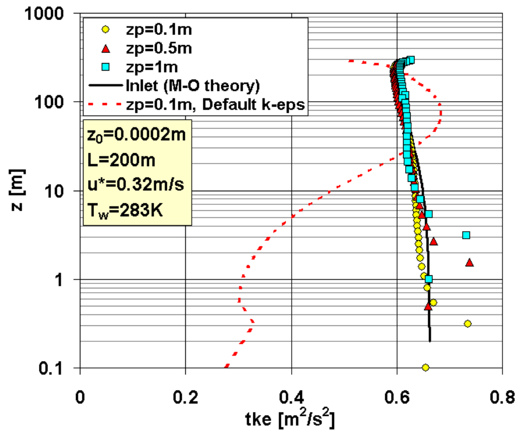

Figure 4: Near-wall grid sensitivity on tke profile. Comparison with default model configuration.

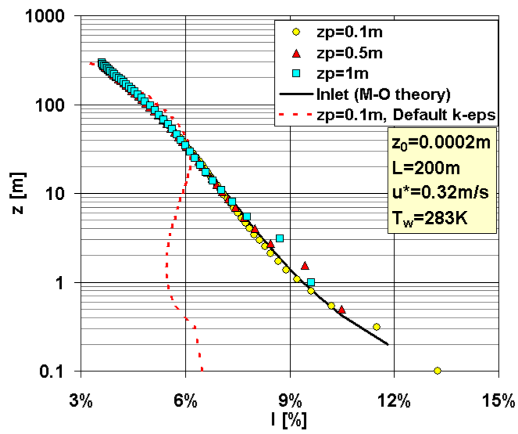

Figure 5: Near-wall grid sensitivity on turbulent intensity. Comparison with default model configuration.

4. On the validity of Monin-Obukhov theory offshore

FINO-1 offshore platform is located 45km off the Borknun Island. A 100-m mast fully equipped with meteorological and oceanographic instruments enables the characterization of atmospheric boundary layer profiles.

Lange [8] compared FINO-1 measurements of mean velocity profiles with those from Rodsand mast in the Baltic Sea, under different stability conditions. The suitability of M-O theory in both cases was studied following reasonably good agreement at both sites under unstable and neutral conditions. In stable conditions, the shorter fetch at Rodsand provided discrepancies with respect to M-O theory, something not noticed at FINO-1.

In the present study, instead of studying the overall mean velocity profiles, segregated by wide stability classes, the analysis is carried out on a localized episode of several days, from the 17th to the 19th of April 2005. Figure 6 shows the evolution of velocity, wind direction, turbulence intensity, air temperature difference and M-O length. The wind direction, rather uniform in the whole period, is coming from the South, where more significant diurnal variability is found due to the influence of the coast. Unstable conditions develop during the night, when the sea temperature is higher than the overlying air. On the contrary, during the day stable conditions appear due to the cooling effect of the sea. The stability is apparent in the turbulence intensity which presents much lower values in stable conditions.

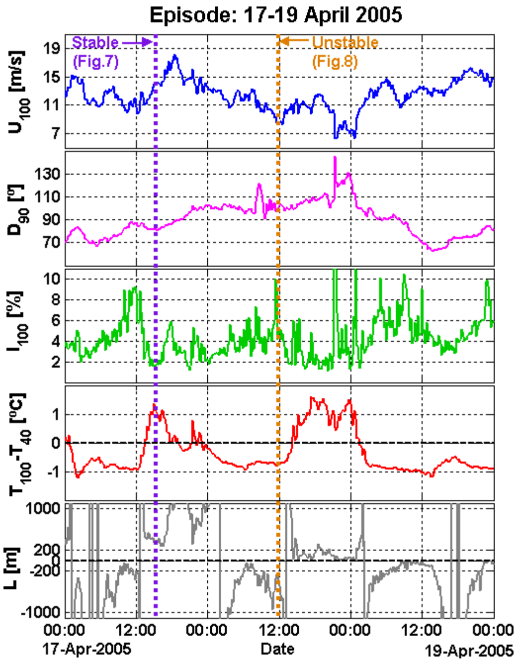

Figure 6: 17-19 April 2005 episode at FINO-1.

The validity of M-O profiles is tested in two 2-hr periods with different stability conditions. Periods of rather stationary behavior have been selected, from which the average profiles are obtained and the M-O best fits are estimated. Figure 7 presents the stable case and Figure 8 the unstable case, both indicated in Figure 6. Together with the M-O best-fit, obtained for the mean *L*, expressions for 0.5*L* and 2*L* are also plotted to show the dependency on this parameter, which is more important in the stable case.

Considering the value of *L* computed from (12) and (13), *L*=-603m, the unstable case is fairly well fitted to M-O profile with a friction velocity of 0.26m/s.

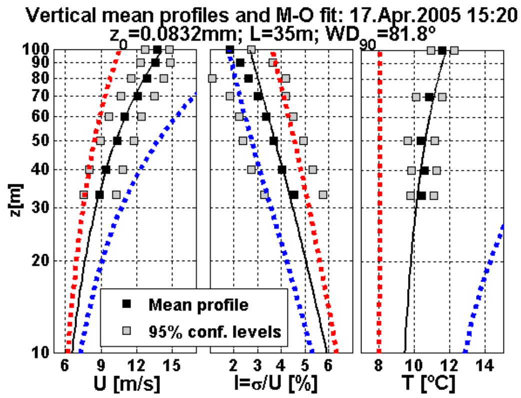

Figure 7: Stable case mean velocity and turbulence intensity profiles with M-O fit.

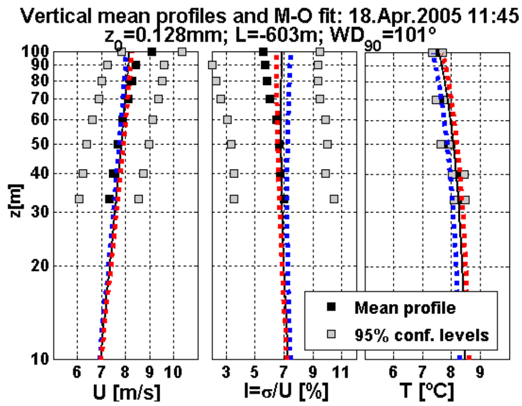

Figure 8: Unstable case mean velocity and turbulence intensity profiles with M-O fit.

On the other hand, tor the stable case, the measurements don't fit to M-O theory with the computed value of *L*=367m, but rather to a much lower value of *L*=35m (with u*=0.22m/s). The discrepancy is attributed to costal effects, as described by Lange et al. [6]: very high temperature differences between advected air from land and sea surface generate a very stable internal boundary layer with low turbulence (2-4%)

and slow growth. A strong inversion is observed at 50m separating the fully developed profile close to the sea surface from the very stable IBL.

5. Conclusions

A CFD k-ε model for the simulation of thermally stratified flows in the atmospheric surface layer is presented. Some preliminary results show the modeling methodology. It is based on M-O similarity theory, which is especially suited for the simulation of offshore wind conditions due to the surface uniformity.

The presented modeling methodology constitutes the basis for the development of a more generalized CFD model for wind resource assessment. Further works will be devoted to solution of the entire boundary layer depth making a link between surface layer M-O theory and geostrophic drag law. Once an equilibrium turbulence model is defined, the next effort will be devoted to the downscaling of mesoscale data in the definition of CFD boundary conditions for high-resolution wind mapping.

Considering the validity of M-O theory in offshore conditions, it has been seen that the application of such theory in particular events is not straightforward in the presence of stable conditions.

References

[1] Alinot C., Masson C., 2005, k-ε Model for the Atmospheric Boundary Layer Under Various Thermal Stratifications, *Transactions of the ASME* **127**, 438-443.

[2] Brodeur P., Masson C., Sibuet-Watters C., Numerical simulations of wind distributions over very complex terrain, *44th AIAA Aerospace Sciences Meeting and Exhibit*, Jan-2006, Reno, Nevada (US).

[3] Blocken, B., Stathopoulos, T., Carmeliet J., CFD simulation of the atmospheric boundary layer – wall function problems. *Atmospheric and Environment* **41-2**, 2007, 238-252.

[4] Cabezón D., Sanz J., van Beeck J. Sensitivity analysis on turbulence models for the ABL in complex terrain. *EWEC-07 Scientific preceedings*, Milan, May 2007.

[5] Dalpé B., Masson C. Recommended practices when analyzing wind flow near a forest edge with WAsP. *EWEC-07 Scientific preceedings*, Milan, May 2007.

[6] Lange B., Larsen S., Hojstrup J., Barthelmie R. Importance of thermal effects and sea surface roughness for offshore wind resource assessment. *Journal of Wind Engineering and Industrial Aerodynamics* **92** (2004), 959-988.

[7] Lange B., Larsen S., Hojstrup J., Barthelmie R., Evaluation of the wind-resource estimation program WAsP for offshore applications, *Journal of Wind Engineering and Industrial Aerodynamics* **89** (2001), 271-291.

[8] Lange B., Comparison of wind conditions of offshore wind farm sites in the Baltic and North Sea, *DEWEC-04 Proceedings*, 2004.

[9] Fluent Inc., Fluent 6.3 User's Guide, *Fluent Inc.*, Lebanon, September 2006.

[10] Franke, J., Hirsch, C., Jensen, A.G., Krüs, H.W., Schatzmann, M., Westbury, P.S., Miles, S.D., Wisse, J.A., Wright, N.G., 2004. Recommendations on the use of CFD in wind engineering. *Proceedings of the International Conference on Urban Wind Engineering and Building Aerodynamics*, in: van Beeck JPAJ (Ed.), COST Action C14, Impact of Wind and Storm on City Life Built Environment, von Karman Institute, Sint-Genesius-Rode, Belgium, 5 - 7 May 2004.

[11] Bechmann A., Sorensen N.N., Johansen J. Atmospheric Flow over Terrain using Hybrid RANS/LES. *EWEC-07 Scientific proceedings*, Milan, May 2007.

[12] Panofsky H.A., Dutton J.A., Atmospheric Turbulence, Models and Methods for Engineering Applications, *Wiley & Sons*, 1984.

[13] Richards P.J., Hoxey R.P., Appropriate boundary conditions for computational wind engineering models using the k-ε turbulence model, *Journal of Wind Engineering and Industrial Aerodynamics* **46-47** (1993), 145-153.